Estimation of Agitator Flow Shear Rate

Jie Wu, Lachlan J. Graham, and Nabil Noui Mehidi
Fluids Engineering Research Laboratory, Commonwealth Scientific and Industrial Research Organization (CSIRO), Highett 3190, Victoria, Australia

DOI 10.1002/aic.10857
Published online April 7, 2006 in Wiley InterScience (www.interscience.wiley.com).

Laboratory laser Doppler velocimetry (LDV) measurements were conducted to measure the shear rate coefficient K_S of a range of impellers. Equations correlating K_S with N_Q (flow number) are provided for axial flow and radial flow impellers. Theoretical formulations based on the classic boundary layer theory are developed to estimate the shear rate at the blade surface. Calculations show that the shear rates at the blade surface are many orders of magnitude higher than those in the flow at the impeller outlet. The software code XFOIL was used to illustrate typical distributions of the shear rates along the blade surfaces. Effects of viscosity, non-Newtonian shear-thinning index, agitator design, and scale-up on shear rates are illustrated. © 2006 American Institute of Chemical Engineers *AIChE J,* 52: 2323–2332, 2006
Keywords: shear rate, shear stress, blade surface, impeller, flow number

Introduction

Shear rate of the flow in a mixing tank is an important parameter controlling many important industrial processes. Shear rate affects the performance of many reacting or nonreacting vessels, such as the growth of alumina hydrate in alumina precipitation reactors and size distribution of resin particles produced in polymerization reactors. It can also have an impact on scale growth. Fundamentally, shear rate affects processes involving mixing Newtonian fluids, non-Newtonian fluids or slurries, generating/dispersing liquid/liquid droplets, and producing fine gas bubbles for gas-to-liquid mass transfer.

Metzner and Otto[1] proposed that the averaged shear rate over the whole tank is proportional to the rotational speed of the impeller, that is,

$$\dot{\gamma} = K_S N \tag{1}$$

where K_S is a nondimensional constant, dependent on impeller geometry, and N is the shaft speed (rev/s). This concept has since been widely accepted and used in non-Newtonian fluid mixing studies.[2-8]

In the original work by Metzner and Otto,[1] the flow of a Rushton turbine operating in two non-Newtonian shear-thinning fluids (CMC and Carbopol water solutions) was studied. The power number vs. Reynolds number was found to match closely with the known Newtonian power number vs. Reynolds number data, when the apparent viscosity was estimated using a single constant K_S of 13. The linear relationship suggested in Eq. 1 was based on the evidence of matching of the power number data, rather than measurement of actual velocity distributions at that time.

In more recent times Torrez and Andre[8] conducted both computational fluid dynamics (CFD) and experimental studies on the velocity profiles at the exit of a Rushton turbine mixing Newtonian and shear-thinning fluids. Their experimental data showed a K_S value of 12.1, whereas their numerical result suggested a lower value of 9.6. In general, literature data[3,9] suggested an approximation of $K_S \approx 11.5$ for a Rushton turbine. Skelland[9] listed K_S data for 45° pitch-bladed turbines and marine impellers.

Shear rates of axial flow impellers were studied by other authors. Weetman and Oldshue[10] presented correlations for power, flow, and shear characteristics of a hydrofoil axial flow impeller (Lightnin A310, SPX Process Equipment, Delavan, WI) and a pitch-bladed turbine, measured through an automated laser Doppler velocimetry (LDV) system. It can be estimated from the averaged velocity gradient data in their article that $K_S = 3.42$ for the Lightnin A310 impeller and $K_S = 5.4$ for the 45° pitch-bladed turbine (down pumping).

Correspondence concerning this article should be addressed to J. Wu at Jie.Wu@csiro.au.

It should be noted that, although the shear rate is defined loosely as an averaged velocity gradient in the impeller region, it is a common practice to calculate the average shear rate at the flow exit plane of impellers, within the impeller diameter periphery. It is therefore proposed here that the shear rate as defined in Eq. 1 be termed average shear rate of impeller *exit flow*, or shear rate at the impeller outlet. The importance of this definition will be made clear later in this article.

Modern process industries use a wide range of commercial impellers with many variations in designs. Known K_S values are limited to only a few traditional impellers. It is one of the purposes of this study to seek to generalize K_S variation with impeller designs, so that rapid estimation can be made at the impeller design stage.

Wu et al.[11] showed, based on solids suspension experiments, that the S factor in the Zwietering's correlation can be generalized to account for variation of impeller design, through a correction using impeller flow number N_Q. One of the purposes of this article is to attempt to use the same philosophy to generalize the effect of varying impeller design on K_S, through using N_Q as the basis for correlation.

Although it may be satisfactory to consider the averaged shear rate at the impeller outlet when correlating power, speed, and other data in Newtonian or non-Newtonian fluid mixing applications, it is not so in some applications where deformation and breakage of bubbles, droplets, particle agglomerates, and biological cells are involved, unless the maximum shear rate is considered. For instances, in liquid–liquid mixing systems, the minimum droplet size is controlled by the *maximum* shear rate, not the *averaged* shear rate. This may have a practical consequence in some processes, such as resin production, because the maximum shear rate can control the amount of the fine resin particles produced from solidification of liquid droplets.

The maximum shear rate is obviously localized on the impeller blade surface. Wichterle et al.[12] is one of the few literature articles that attempts to quantify the maximum shear rate on turbine blades. They used an electrochemical method to measure the shear rate on the front side of a Rushton turbine. They showed that shear rates on the impeller are orders of magnitude higher than the shear rate conventionally assumed using Eq. 1. So far this result has been largely ignored in the literature. It is the main purpose of this article to clarify this important issue, through formulating basic equations to calculate the maximum shear rates on the impeller blades.

Theoretical Analysis

Averaged shear rate at the impeller outlet

The averaged shear rate of the flow at the impeller outlet can be related to the impeller pumping flow rate:

$$K_S = \frac{\langle \dot{\gamma} \rangle}{N} \propto \frac{V/D}{N} \propto \frac{(Q/D^2)/D}{N}$$

where N is the shaft speed, V is the impeller exit velocity, D is the impeller diameter, Q is the impeller pumping flow rate, and $\langle\ \rangle$ denotes averaging.

Given that $Q = N_Q N D^3$, where N_Q is the flow number, we conclude that

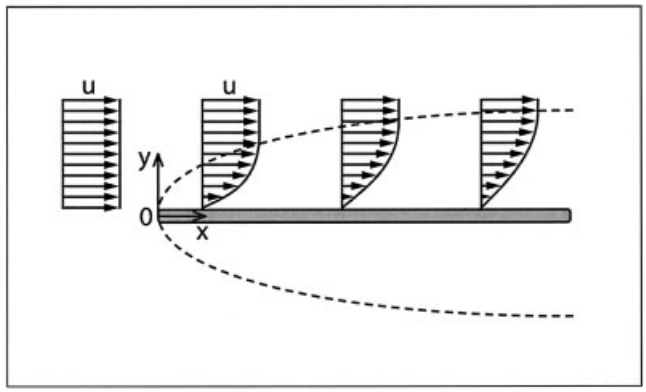

Figure 1. Flow along a flat plate: boundary layer development.

$$K_S \propto N_Q \tag{2}$$

This suggests that K_S is linearly related to the impeller flow number. To determine K_S from experiments, LDV data were processed and the averaged velocity gradient was obtained at the impeller outlet plane, within the periphery of impeller diameter. Refer to Torrez and Andre[8] or Weetman and Oldshue[10] for detailed description.

Shear rate at the blade surface

To determine the surface shear rates it is necessary to calculate the shear stress at the blade surface:

$$\dot{\gamma} = \frac{\tau}{\mu} = \frac{C_f \rho u^2}{2\mu} = \frac{C_f u^2}{2\nu} \tag{3}$$

where C_f is the surface skin friction coefficient:

$$C_f = \frac{2\tau}{\rho u^2}$$

where τ is the shear stress at the blade surface; μ and ν are the dynamic and kinematic viscosities, respectively; u is the free stream velocity; and ρ is the fluid density.

Flat plate aligned in the flow direction

Without losing its general significance, we will consider calculating the averaged shear rate at the surface of a thin flat plate, aligned to the flow direction (Figure 1). It is recognized that C_f varies along the blade, typically decreasing as the distance from the leading edge increases (to be discussed later). The averaged skin coefficient can be expressed in terms of the drag coefficient C_D because the pressure-difference–related form drag is neglected here (thin flat plate assumption):

$$\dot{\gamma}_{mean} = C_D \frac{u^2}{2\nu}$$

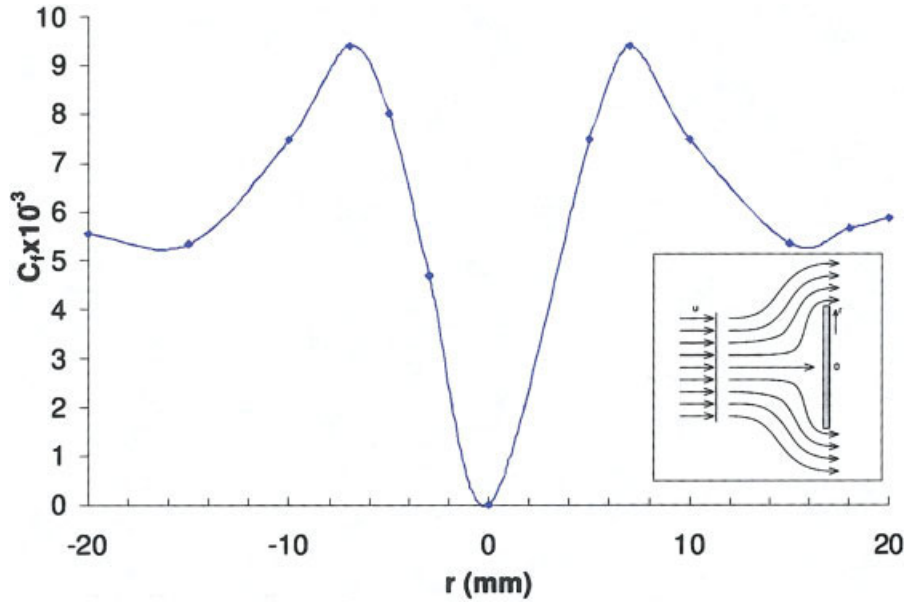

Figure 2. Skin coefficient distribution along a plate normal to an impinging jet, where *r* is the distance from the jet center; Re = 41,600.

Data courtesy of Alekseenko and Markovich.[16] [Color figure can be viewed in the online issue, which is available at www.interscience.wiley.com]

where the subscript *mean* denotes averaged along the blade (thin flat plate). Also it is noted here that the drag coefficient C_D is for only one side of the plate.

Using the classic boundary layer theory,[13,14] averaged shear rates on the surface of a thin plate, aligned in the flow direction, can be found:

- For laminar flow:

$$\dot{\gamma} = 0.664 \frac{u^{1.5}}{\sqrt{(c\nu)}} \tag{4a}$$

- For turbulent flow:

$$\dot{\gamma} = (0.004 - 0.01) \frac{u^2}{2\nu} \tag{4b}$$

where c is the chord length of a blade section; the drag coefficient for turbulent flow has a range, which is dependent on the surface roughness and, for simplicity, the subscript *mean* is removed here.

For non-Newtonian shear-thinning fluids described by the power law:

$$\tau = K\dot{\gamma}^n \tag{5}$$

where K is the non-Newtonian consistence index and n is the flow behavior index. The averaged shear rate at the surface of plate in laminar regime as described by Eq. 4a can be modified using the relationship Eq. 5, resulting in an expression of the shear rate for a non-Newtonian power-law fluid, in the laminar flow regime:

$$\dot{\gamma} = \left(0.664 \frac{u^{1.5}}{\sqrt{(c/\rho)}}\right)^{2/(n+1)} \frac{1}{K^{n+1}} \tag{6}$$

We have in effect inserted a non-Newtonian apparent viscosity into the Newtonian drag Eq. 4a, assuming the basic form of the drag coefficient equation established in Newtonian flow remains valid, simplifying a reported more complicated influence by the non-Newtonian effect.[15]

Plate normal to the flow direction

The boundary layer on the flow normal to a plate is difficult to quantify analytically. Alekseenko and Markovich[16] measured the shear stress along a plate normal to an impinging jet using an electrical diffusion technique. A typical skin friction coefficient distribution result based on their measurement is shown in Figure 2. The maximum skin friction is $C_f \approx 0.0095$, at Re = 41,600. As an approximation, this will be used later to estimate the shear rate at a Rushton turbine blade surface in the turbulent flow regime.

Experimental Setup

The model mixing rigs (Figure 3) consist of a T = 390 mm diameter tank (T390) and a T = 1070 mm diameter tank (T1070), both with flat bottoms, placed inside rectangular outer glass/acrylic tanks. The outer tanks are filled with water to minimize optical distortion. Four baffles (1/12)T in width and equally spaced were installed in the circular tanks. Test impellers, with D/T in the range of 0.33–0.49, were mounted on the central shafts equipped with torque transducers and speed detectors (Ono Sokki, Yokohama, Japan). The speed and torque were logged using a personal computer equipped with a suitable data acquisition board and provided on-line analysis of power consumption and other parameters.

Velocity distributions were measured in the model mixing vessels using a two-dimensional optical-fiber LDV system

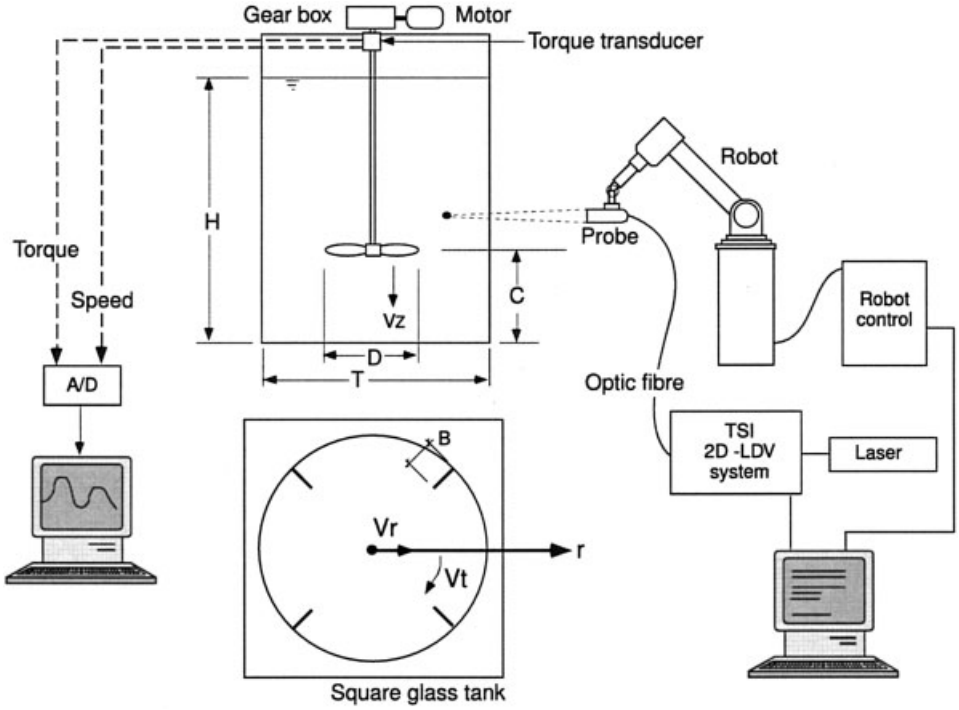

Figure 3. Mixing tank and laser Doppler velocimetry (LDV) measurement system.

The LDV probe was mounted on a robotic arm with a positioning resolution of 0.1 mm.

(TSI, Shoreview, MN). The LDV probe, which has built-in transmitting and receiving optics, was mounted on an industrial robotic arm, allowing the crossing point of the laser beams to be automatically positioned within the tank. The time–mean velocity data thus obtained were found repeatable to within 1%. Time–mean statistics of the velocity data were obtained using a measuring volume transit time-weighted bias correction method incorporated in the TSI software package. Tap water and glycerol water solutions were used as the working fluids in the experiments.

Computational Simulation

Calculations of distribution of skin friction coefficient along aerofoil blade sections were done using the software code XFOIL, based on the panel method.[17] A viscous formulation in the code was used during the calculations, which includes calculations of the boundary layer and its coupling with the external potential flow solution. The present calculations were performed for a Reynolds number of 10^6.

Results

Averaged shear rate: correlation with flow number

Figure 4 shows correlation of K_S with N_Q for both radial and axial flow impellers. The data were obtained by calculating the averaged gradient of the velocity distributions at the impeller outlet planes. The calculations were performed numerically:

- Axial flow impellers

$$\dot{\gamma} = \frac{\Sigma \left(\frac{\Delta V}{\Delta r}\right)_j V_j r_j \Delta r}{\Sigma\, V_j r_j \Delta r} \tag{7a}$$

- Radial flow impellers

$$\dot{\gamma} = \frac{\Sigma \left(\frac{\Delta V}{\Delta z}\right)_j V_j \Delta z}{\Sigma\, V_j \Delta z} \tag{7b}$$

where the summations were carried out within the periphery of the impeller blades; V is the axial velocity in Eq. 7a, or radial velocity in Eq. 7b; r is the radial distance from the axis; z is the vertical distance; and the subscript j denotes the jth measurement point.

Refer to Wu et al.[11] for more detailed velocity measurement information. Data from Skelland[9] and Weetman and Oldshue[10] are also included for comparison, showing good agreement in general.

The data confirm the formulation Eq. 2, illustrated earlier, that is, K_S is linearly related to the impeller flow number.

It is recommended that the following approximations be used for estimation:

- For axial flow impellers

$$K_S \approx 7N_Q \tag{8a}$$

- For radial flow impellers

$$K_S \approx 14N_Q \tag{8b}$$

Dyster et al.[18] showed, based on LDV measurements on a Rushton turbine in a Newtonian fluid, that impeller flow number N_Q decreases as Reynolds number is reduced.

Figure 5 shows our results for axial hydrofoil impellers (Lightnin A310), obtained based on LDV measurements using glycerol–water solutions over a wide range of Reynolds numbers. It shows that a similar dependency of flow number on Reynolds number exists for axial flow impellers at low Reynolds number, and constant at higher Reynolds numbers (such as $\mathrm{Re} > 10^5$).

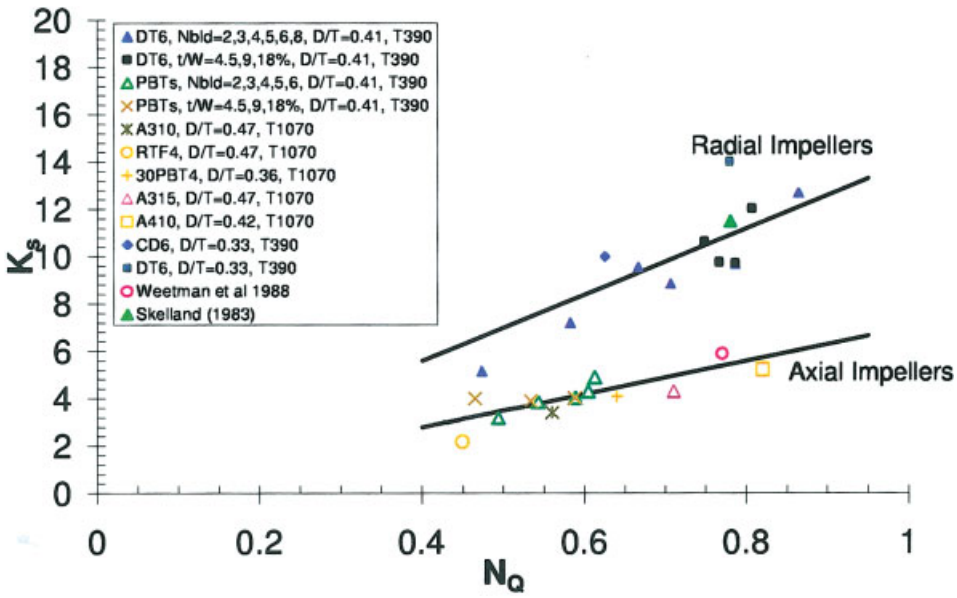

Figure 4. Shear coefficient variation with impeller flow number, turbulent flow data.

Measurements carried out in T390 and T1070 tanks in water. N_{bld} denotes the number of blades, t denotes the blade thickness, and w denotes the blade width. [Color figure can be viewed in the online issue, which is available at www.interscience.wiley.com]

Figure 6 shows variation of K_S with Reynolds number. The data clearly suggest that K_S is not a constant, as conventionally assumed. The prediction using Eq. 8 and the relationship between N_Q and Re is also included in the figure, in reasonable agreement with measurements.

In general, the present results suggest that when N_Q starts to decrease substantially below the turbulent value at low Reynolds numbers, a correction on K_S should be carried out using Eq. 8, whereas in the turbulent flow regime K_S can be taken as a constant, independent of Reynolds number, given that N_Q is practically constant in turbulent flows.

Shear rate at the blade surface

The purpose here is to evaluate the maximum shear rate that occurs at the blade surface at the impeller tip. To use Eqs. 4a, 4b, and 6 to calculate the shear rate at the impeller blade surface, it is necessary to determine the flow velocity relative to the rotating impeller blade. By reference to the velocity triangle analysis by Wu and Pullum,[19] it can be shown* that

$$V \approx U_{tip}\sqrt{\left[1+\left(\frac{4N_Q}{\pi^2}\right)\right]^2} \tag{9}$$

where V is the velocity relative to the rotating blade (impeller tip) and U_{tip} is the impeller tip velocity, for axial flow impeller.

For radial flow impellers, it is a close approximation to assume $V = U_{tip}$.

Shear Rate Variation with Speed: Turbulent Regime. Fig-

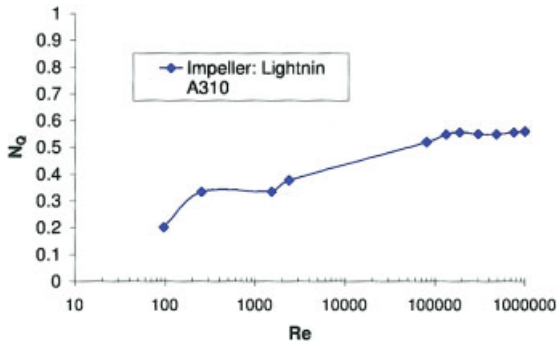

Figure 5. Flow number variation with Reynolds number: Lightnin A310 impeller, installed pumping downward.

Tank diameters = 390 and 1070 mm; impeller diameter D = 161, 193, and 452 mm. Installed typically at C = 1/3 of tank diameter. Fluid: water and glycerol of various concentrations. [Color figure can be viewed in the online issue, which is available at www.interscience.wiley.com]

* Here the contribution from the swirling velocity component is neglected because it is typically significantly smaller than the tip velocity.

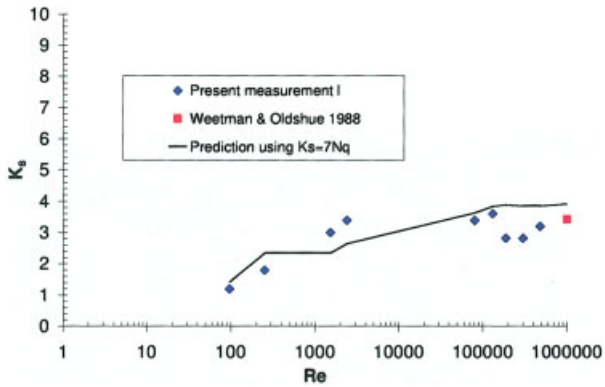

Figure 6. Effect of varying Reynolds on K_S.

Prediction data made using $K_S = 7N_Q$. Impeller used Lightnin A310. [Color figure can be viewed in the online issue, which is available at www.interscience.wiley.com]

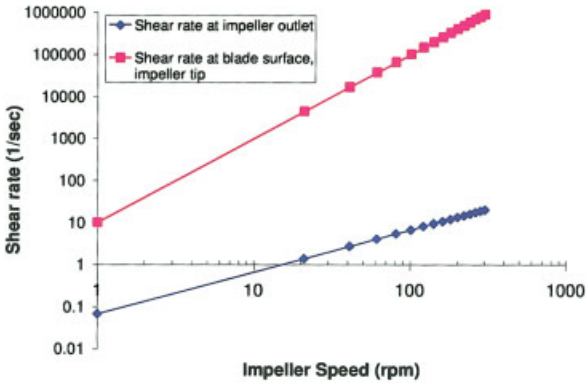

Figure 7. Shear rate variation with speed *N* of a down pumping 30° pitch, four-bladed turbine; blade width is 1/5 of impeller diameter, denoted as 30PBT4.

Diameter $D = 1$ m. Fluid: water; flow is in Newtonian turbulent regime. $C_D = 0.007$. [Color figure can be viewed in the online issue, which is available at www.interscience.wiley.com]

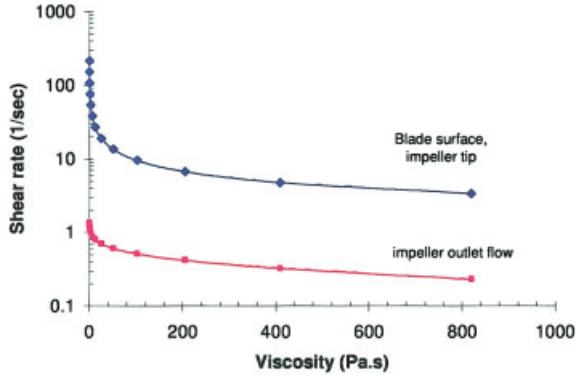

Figure 9. Shear rate variation with viscosity.

Calculation case: a downward pumping 30PBT4 turbine, with diameter of 1 m and operating at 30 rpm. Fluid: Newtonian liquid with viscosity ranging from 0.2 to 810 Pa·s. [Color figure can be viewed in the online issue, which is available at www.interscience.wiley.com]

ure 7 shows calculated shear rates of a 30° pitch, four-bladed turbine (30PBT4, diameter of 1 m), pumping downward in a Newtonian turbulent flow regime. It can be seen that the shear rate at the blade surface (located at the impeller tip) is many orders of magnitude higher than that in the flow at the impeller exit, as predicted by the conventional assumption using Eq. 1, with $K_S = 4.1$. It can also be seen that the former increases considerably faster than the latter with speed because the former is a function of N^2 and the latter is a function of N in turbulent flow regimes (refer to Eqs. 4b and 1).

Figure 8 shows shear rate calculation results for a Rushton turbine (diameter of 1 m) operating in water in the turbulent regime, based on the maximum skin coefficient of $C_f = 0.0095$ (refer to Figure 2). Again, the blade surface shear rate is calculated at the impeller tip. The results calculated for the pitch-bladed turbine (Figure 7) are plotted in dotted lines for comparison, showing essentially similar trends and characteristics. Again it can be concluded that for a radial turbine, the shear rate at the blade surface is considerably higher than that in the flow at the impeller outlet.

Shear Rate Variation with Re: Newtonian and Non-Newtonian Laminar Flows. Figure 9 shows variation of shear rate of the 30PBT4 (30° pitch, four-bladed turbine) with viscosity in a Newtonian laminar flow regime. The calculation was undertaken while keeping the impeller (diameter of 1 m) speed at 30 rpm, and the Newtonian viscosity was varied from 0.2 to 800 Pa·s. It can be seen that shear rates generally decrease with increasing viscosity. It can also be seen that the shear rates at the blade surface are orders of magnitude higher than those in the flow at the impeller outlet, similar to those found in the turbulent flow regime.

Again, as presented in the previous section, it can be concluded that both shear rates at the blade surface and at the impeller exit flow are dependent on Reynolds number, in the laminar flow regime.

Figure 10 shows variation of the shear rate at the blade surface (impeller tip) of the same 30PBT4 with the non-

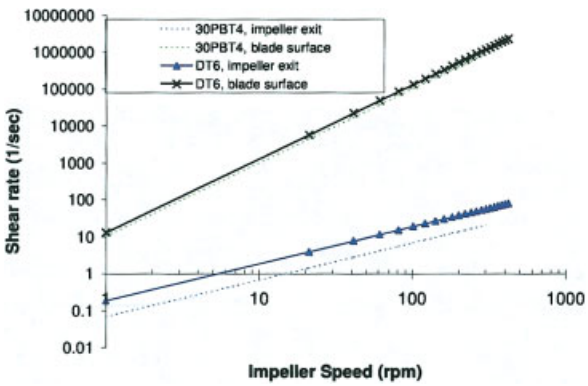

Figure 8. Shear rate variation with speed *N* of a six-bladed Rushton turbine.

Diameter $D = 1$ m. Fluid: water; flow is in Newtonian turbulent regime. [Color figure can be viewed in the online issue, which is available at www.interscience.wiley.com]

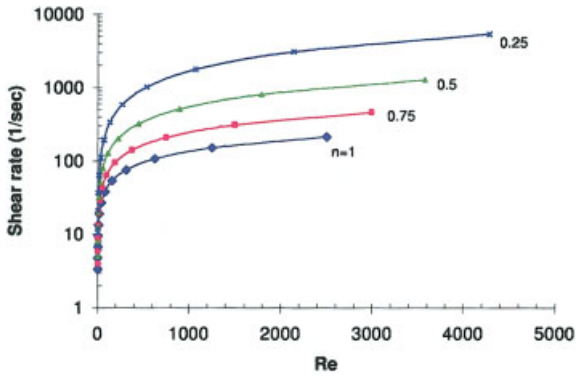

Figure 10. Shear rate variation with the generalized Reynolds number at different flow indices.

Calculation cases: a downward pumping 30PBT4 turbine, with diameter of 1 m and operating at 30 rpm. Fluid: power-law non-Newtonian fluid. [Color figure can be viewed in the online issue, which is available at www.interscience.wiley.com]

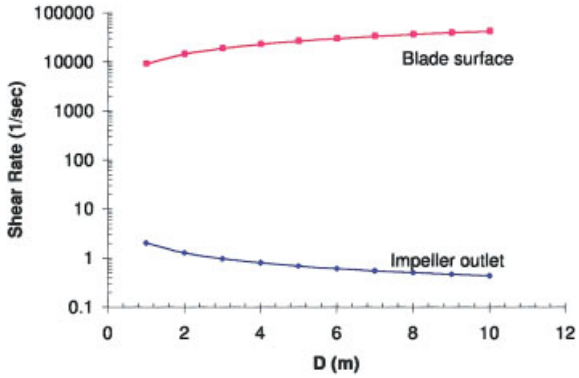

Figure 11. Shear rate variation on scaling-up based on constant power per unit volume.

Impeller: downward pumping 30PBT4 turbine. At diameter of 1 m, impeller speed is 30 rpm. Turbulent flow, viscosity = 0.001 Pa·s. [Color figure can be viewed in the online issue, which is available at www.interscience.wiley.com]

Newtonian generalized Reynolds number (power-law fluids), defined as

$$\mathrm{Re} = \frac{\rho N^{2-n} D^2}{K K_s^{n-1}} \tag{10}$$

where K and n are power-law indices, defined in Eq. 5. For Newtonian flow, $n = 1$, corresponding to the lowest curve in Figure 10. It can be seen that shear rate at the blade surface increases as n decreases. This suggests that the non-Newtonian shear-thinning effect tends to increase the shear rate at the blade surface, which is consistent with the common knowledge that the velocity gradient increases with the increasing non-Newtonian shear-thinning effect (reduction in n). As an example, readers are referred to Collins and Schowalter[20] for a case on non-Newtonian fluids flowing through a channel.

Shear Rate on Scale-up. Scaling-up of laboratory test results is often practiced for full-scale design. It is of major interest to examine variation of shear rates as the design is scaled-up. Many scale-up rules may be used, such as constant power per unit volume, constant tip velocity, and so forth. For the purpose of illustration, the constant power per unit volume rule will be used here:

$$\frac{P}{Vol} \propto \frac{\rho N^3 D^5}{D^3} = \rho N^3 D^2 = \text{const} \tag{11}$$

Figure 11 shows the calculation results of the 30PBT4 scaled from a diameter of 1 m operating at 30 rpm up to a maximum diameter of 10 m, based on constant power per unit volume, for turbulent flow (water). It can be observed that the shear rate at the impeller outlet generally decreases on scaling-up. On the other hand, the shear rate at the blade surface increases in turbulent flow on scaling-up; this is not usually conventionally assumed.

Shear Rate Control through Impeller Design. Sometimes it is of practical interest to design a mixing system to control the maximum shear rates. For example, one may want to minimize the maximum shear rate in a mixing tank, to reduce the amount of fine droplets produced in a liquid/liquid mixing system, while still maintaining a required mean droplet size. This can be achieved by altering the impeller design, such as varying the pitch angle or changing the number of blades, while maintaining the same power input.

Table 1 shows a list of measured flow number, power number of a number of pitch-bladed turbines, and a Lightnin A310 impeller. The speed was varied to keep the power consumption constant for all the impeller designs. It can be seen that flow shear rate at the impeller outlet (based on measured K_S) varies only marginally, suggesting that the shear rate of bulk flow in the tank remains relatively unchanged when different axial flow impellers were used at the same power input. On the other hand, the shear rate at the blade surface (impeller tip) decreases as more "heavy duty" impellers (that is, with increasing power number) are used, while maintaining the same power input.**

The present result suggests that the maximum shear rate (which occurs at the blade surface at the impeller tip) can be reduced through impeller design modification, while providing the same mean bulk flow shear rates and flow circulation requirement (that is, using the same power input).

Shear Rate (Stress) Variation along the Blade Surface. So far, averaged shear rate along the blade surface has been considered based on the total skin friction coefficient (that is, drag coefficient C_D); variation of the shear rate along the blade surface has been ignored. In reality, shear stress at a blade surface varies with distance from the leading edge of the blade. As an illustration, an aerofoil section NACA 4412 and a thin flat plate (actually a NACA 0006 profile to allow for numerical solution) were analyzed using the software code XFOIL. The skin coefficient distribution along the NACA 4412 aerofoil is shown in Figure 12, for the case of flow approaching the aerofoil at a zero angle of attack. The Reynolds number based on the free stream velocity and the aerofoil chord length c is 10^6.

It may be concluded in general that the peak shear stress/shear rate ($=\tau/\mu$) occurs at the leading edge of a blade; moreover, it generally decreases along the surface away from the leading edge. It is also interesting to note that, in the test calculation case, the skin friction coefficients rapidly increase

** This is roughly equivalent to maintaining the same pumping flow for pitch-bladed turbines, as shown in Wu et al.[11]

Table 1. Shear Rate Variation with Power Number*

					$\dot{\gamma}$ (1/s)	
Impeller	N_Q	P_0	N (rpm)	P (W)	Impeller Outlet	Tip Blade Surface
20PBT4	0.43	0.27	300	3.6	15.1	23,371
A310	0.56	0.32	284	3.6	18.5	20,869
25PBT4	0.37	0.53	253	3.6	16.7	18,944
30PBT2	0.45	0.49	253	3.6	14.5	16,626
30PBT4	0.59	0.56	235	3.6	16.2	14,371
40PBT4	0.72	0.97	196	3.6	16.4	9,964
45PBT4	0.76	1.22	181	3.6	16.1	8,551

*Power, flow, and impeller outlet shear rate data were measured in a T390 tank operating in water, tank diameter 390 mm, impeller diameter 160 mm, impeller to tank bottom distance 130 mm, water level 400 mm. The shear rates at the blade surfaces were calculated using Eq. 4b, $C_D = 0.007$. The relative blade thickness of PBTs was 0.047, normalized by the blade chord length.

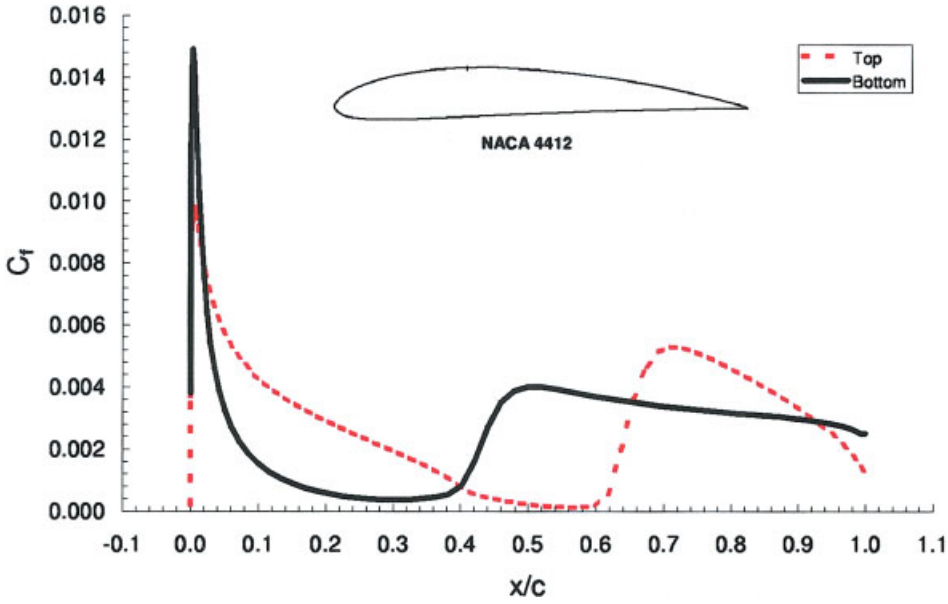

Figure 12. Skin friction coefficient variation along a NACA4412 aerofoil, at a Reynolds number of 10^6.

The angle of attack is zero, x is the surface distance from the leading edge, c is the chord length. Calculated using the XFOIL code. [Color figure can be viewed in the online issue, which is available at www.interscience.wiley.com]

to higher values before decreasing again, at a distance x/c = 0.4–0.6. This increase in skin friction is related to a transition from laminar to turbulent boundary layer flow.

Integration of the skin friction distribution expressed in C_{Df} is shown in Figure 13, as a function of the angle of attack, for both the NACA 4412 aerofoil and the thin flat plate. The data are equivalent to the drag coefficient excluding the form drag component (by the pressure difference). To assess deviation of the peak values from the averaged values, the ratio of the peak stress over the averaged stress was determined to be in the range of 3–5. The result of this estimation may be used as a rough guide when assessing the peak shear rates on the blade surface.

The effect on C_{Df} of varying the angle of attack of the flow approaching the blades is relevant to axial flow impellers.† Readers are referred to Wu and Pullum[19] for detailed analysis on the flow field relative to a rotating blade. Here it is of interest to note that the minimum C_{Df} corresponds to when the approaching flow is fully aligned with the blade. An increase or a reduction in the angle leads to an increase in C_{Df}; however, C_{Df} decreases if the angle is deviated too far away from zero, corresponding to the condition of reduced surface shear stress (thus shear rate) at flow separation.

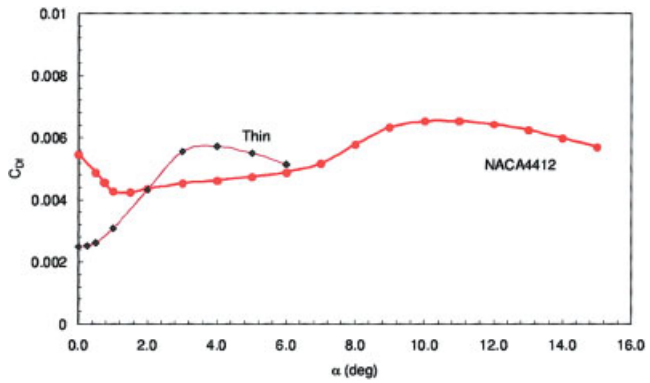

Figure 13. Variation of integrated skin coefficient with angle of attack, calculated using the XFOIL code at a Reynolds number of 10^6.

Blade sections: NACA4412 aerofoil, thin plate with leading edge rounded, and trailing edge tapered (actually NACA 0006 profile). [Color figure can be viewed in the online issue, which is available at www.interscience.wiley.com]

Discussion

The shear rate coefficient K_S has been conventionally assumed to be independent of viscosity since originally introduced by Metzner and Otto.[1] They justified this assumption based on a successful fitting (within an accuracy of 15%) of the power data of a Rushton turbine over a wide range of Reynolds numbers, using a single constant K_S. This has since been accepted and used by most authors, perhaps because of its convenience. In recent years, many LDV velocity measurements on mixing tank flows have been reported in the literature, but few attempted to quantify K_S.

The present work shows that K_S data are proportionally correlated with impeller flow numbers. Because flow number data are usually well documented for most impeller designs, it is hoped that this finding will make it easy to estimate the K_S value of any given impeller, based on our recommended Eqs. 8a and 8b. It is known that flow number varies with Reynolds number; that is, in the laminar flow regime, it decreases as the Reynolds number is reduced. It is therefore not surprising to see that K_S decreased as viscosity was increased in experiments, using glycerol–water solutions, and operating the agi-

† Generally speaking, the angle of attack of the flow approaching the blades is substantially smaller than the blade pitch angle of an axial flow impeller (refer to Wu and Pullum[19]).

tator (a Lightnin A310 axial flow impeller) at a fixed speed. This new finding of dependency of K_S on Reynolds number is based on a limited amount of experimental data. It is recommended that more measurements or CFD simulations be conducted in the future to correlate the effect of Reynolds number on K_S.

The present results show that the shear rates at the blade surface are typically many orders of magnitude higher than those found in the bulk flow, such as at the impeller outlet. It is hoped that this finding will provide a useful new perspective to analyze many important mixing applications. For example, to control the shear damage on culture cells growing in a bioreactor, it would make most sense to estimate the maximum shear rate at the blade surface during the design process. If necessary, the maximum shear rate could be minimized to avoid cell damage, through modifying impeller design parameters. This is actually possible as illustrated in this article, that if a "heavy duty" impeller is used, a significantly lower shear rate at the blade surface can be achieved, while maintaining the same power input.

In passing, it may be interesting to comment that on scaling-up (based on constant power per unit volume), the shear rates at the blade surface generally increase as shown in this study. This conclusion may vary depending on the scaling-up rules and the flow regime. For example, it can be seen by inspecting Eqs. 4a and 6 that in the viscous laminar flow regime, for both Newtonian and non-Newtonian power-law flows, shear rate at the blade surface will decrease if scaling-up is based on constant impeller tip velocity. On the other hand, for high Reynolds number turbulent flows, the shear rates will remain constant when scaling-up on constant impeller tip velocity (refer to Eq. 4b).

Adding to the complexity is the variation of the shear rate (or shear stress) along the blade surface, as illustrated by the computational simulation based on a panel method, which coupled boundary layer solutions with the external potential flow field. It is interesting to note that the shear rates peaked near the leading edge of a blade, on both sides of the blades. Sample calculations (not shown in this article) indicated that it is possible to minimize the peak shear rates through modifying the airfoil profiles. This is left for further study in the future.

Conclusions

Experimental data were used to show that the shear rate coefficient K_S is linearly correlated to impeller flow number. Equations correlating K_S with N_Q are provided for axial flow and radial flow impellers. Measurements showed that increasing viscosity in the laminar flow regime led to reduction in K_S. This can be conveniently accounted for by using the correlation between flow number and Reynolds number. Equations based on the classic boundary layer theory are developed to estimate the shear rate at the blade surface. Calculations show that the shear rates at the blade surface are many orders of magnitude higher than those in the flow at the impeller outlet. A software code XFOIL was used to illustrate typical distributions of the shear rates along the blade surfaces. The effect of viscosity, non-Newtonian shear-thinning index, agitator design, and scale-up on shear rates are illustrated.

Notation

C = impeller to tank bottom clearance, or blade chord length, m
C_D = drag coefficient
C_{Df} = drag coefficient, arising from the skin friction component
C_f = skin friction coefficient
D = impeller diameter, m
K = power-law consistency index, Pa·s^{-n}
K_S = impeller shear coefficient
LDV = laser Doppler velocimetry
n = power-law flow index
N = shaft speed, rpm, rev s^{-1}
N_Q = flow number = $Q/(ND^3)$
P = shaft power, W
$P_.$ = impeller power number = $P/(\rho N^3 D^5)$
##PBT* = standard pitch-bladed turbines, with blade width 1/5 of impeller diameter: ##, pitch angle; *, number of blades
Q = impeller flow rate, m^3 s^{-1}
r = radial distance from the shaft axis, or from blade center, m
Re = Reynolds number = $\rho(ND^2/\mu)$, or Re = $(\rho N^{2-n}D^2/KK_s^{n-1})$ for non-Newtonian power-law fluid
T = tank diameter, m
t = blade thickness, m
T390 = mixing tank with diameter of 390 mm
T1070 = mixing tank with diameter of 1070 mm
u = free stream velocity, m s^{-1}
U_{tip} = impeller tip velocity, m s^{-1}
V = velocity relative to blade, or velocity at the impeller outlet, m s^{-1}
Vol = tank liquid volume, m^3
w = blade width, m
x = the surface distance from the leading edge of a blade, m

Greek letters

α = angle of attack, degrees
$\dot{\gamma}$ = shear rate, s^{-1}
μ = dynamic viscosity, Pa·s
ν = kinematic viscosity (=μ/ρ), m^2 s^{-1}
ρ = fluid density, kg m^{-3}

Literature Cited

1. Metzner AB, Otto RE. Agitation of non-Newtonian fluids. *AIChE J.* 1957;3:3-10.
2. Nienow AW. Hydrodynamics of stirred bioreactors. *Appl Mech Rev.* 1998;51:3-32.
3. Nienow AW, Elson TP. Aspects of mixing in rheologically complex fluids. *Chem Eng Res Des.* 1988;66:5-15.
4. Ducla JM, Desplanches H, Chevalier JL. Effective viscosity of non-Newtonian fluids in a mechanically stirred tank. *Chem Eng Commun.* 1983;21:29-36.
5. Posarac D, Watkinson AP. Mixing of lignin-based slurry fuel. *Can J Chem Eng.* 2000;78:265-270.
6. Pullum L, Welsh CM, Hamilton N, Ballie K, Kam P. The use of a non-Newtonian fluid to visualize the mixing of a pseudo-homogeneous slurry. *Liquid–Solid Flows 1994: Presented at the 1994 ASME Fluids Engineering Division Summer Meeting, Lake Tahoe, Nevada, June 19–23, 1994*. New York, NY: American Society of Mechanical Engineers Fluids Engineering Division; 1994;189:207-214.
7. Nouri JM, Hockey RM. Power number correlation between Newtonian and non-Newtonian fluids in a mixing vessel. *J Chem Eng Jpn.* 1988;31:848-852.
8. Torrez C, Andre C. Power consumption of a Rushton turbine mixing viscous Newtonian and shear-thinning fluids: Comparison between experimental and numerical results. *Chem Eng Technol.* 1998;21:599-604.
9. Skelland AHP. Mixing and agitation of non-Newtonian liquids. In: Cheremisionoff NP, ed. *Handbook of Fluids in Motion*. Ann Arbor, MI: Ann Arbor Science; 1983;Chap. 7:179-209.
10. Weetman RJ, Oldshue JY. Power, flow and shear characteristics of mixing impellers. Proceedings of the 6th European Conference on Mixing, May 24–26, Pavia, Italy; 1988.

11. Wu J, Zhu Y, Pullum L. Impeller geometry effect on velocity and solids suspension. *Trans IChemE*. 2001;79(Part A):989-997.
12. Wichterle K, Kadlec M, Zak L, Mitschka P. Shear rates on turbine impeller blades. *Chem Eng Commun.* 1984;26:25-32.
13. Schlichting H. *Boundary-Layer Theory*. Reprint. New York, NY: McGraw-Hill; 1979.
14. Blevins RD. *Applied Fluid Dynamics Handbook*. Reprint Edition. Melbourne, FL: Krieger Publishing; 1992.
15. Wu J, Thompson MC. Non-Newtonian shear-thinning flows past a flat plate. *J Non-Newtonian Fluid Mech.* 1996;66:127-144.
16. Alekseenko SV, Markovich DM. Electrodiffusion diagnostics of wall shear stresses in impinging jets. *J Appl Electrochem.* 1994;24:626-631.
17. Drela M. XFOIL: An analysis and design system for low Reynolds number airfoils, in low Reynolds number aerodynamics. In: Mueller TJ, ed. *Lecture Notes in Engineering #54*. New York, NY: Springer-Verlag; 1989.
18. Dyster KN, Koutsakos E, Jaworski Z, Nienow AW. An LDA study of the radial discharge velocities generated by a Rushton turbine: Newtonian fluids, Re $\geq$ 5. *Trans IChemE.* 1993;71(Part A):11-23.
19. Wu J, Pullum L. Performance analysis of axial flow mixing impellers. *AIChE J.* 2000;46:489-498.
20. Collins M, Schowalter WR. Behaviour of non-Newtonian fluids in the inlet region of a channel. *AIChE J.* 1963;9:98-102.

Manuscript received Aug. 21, 2005, and revision received Mar. 5, 2006.